Available online at www.sciencedirect.com
SCIENCE DIRECT®
Journal of Organometallic Chemistry 690 (2005) 2638–2643
Journal of Organometallic Chemistry
www.elsevier.com/locate/jorganchem

Impact of anionic substitutions on apatite structure and properties

Mihkel Veiderma *, Kaia Tõnsuaadu, Rena Knubovets, Merike Peld

Department of Chemical Engineering, Tallinn University of Technology, Ehitajate Tee 5, Tallinn 19086, Estonia

Received 12 July 2004; accepted 12 November 2004
Available online 11 February 2005

Abstract

A review of the results of the authors on single and coupled substitutions of F for OH, and of CO_3 and SO_4 for PO_4 in synthetic and natural apatites, their influence on apatite structure and properties, studied by peak fitting FTIR, XRD, TG/DTA and TG/EGA methods, is presented. Calcination of carbonate and sulphate substituted apatites leads to the formation of stable stoichiometric apatite.

Keywords: Apatite; Fluorhydroxy-; Carbonate-; Sulphate-; FTIR; XRD; TG/DTA; TG/EGA

1. Introduction

Apatite is a basic mineral of phosphate ores as well as a component of bones and teeth of vertebrates. Apatites have found use in several applications such as sorbents, catalysts, and biomaterials. The structure and chemistry of apatites is thoroughly reviewed by Elliot [1,2].

Apatites may contain several different substituents in their structure. The properties of apatites depend on the nature of monovalent anion, substitutions for PO_4 groups and cationic sites (especially in Ca II position) [3].

In this paper the results of a research of the authors on the impact of anionic substituents, singly and coupled, on the structure and properties of natural and synthetic calcium apatites are presented.

2. Fluorhydroxy-apatites and hydrogen bond

Natural apatites (in particular the magmatic ones) are usually fluorhydroxy-apatites (FOHAp) with variable F:OH ratio: $Ca_{10}(PO_4)_6F_n(OH)_{2-n}$. Anomalies in the behaviour of natural and synthetic FOHAps in thermal, dissolution and adsorption processes have been established, manifested by their lower reactivity in comparison with pure F- or OH-apatites. For example, the studies on the hydrothermal processing of FOHAp revealed that in the course of the reaction the degree of defluorination remains lower than the decomposition rate of the apatite, thus fluorine is remained in the structure [4]. These phenomena are explained by the existence of strong OH–F hydrogen bonding in apatite structure.

The presence of OH bonding can be detected by IR spectroscopy in the domain of the OH stretching mode at 3500–3600 cm^{-1} and the libration OH mode at 630 cm^{-1}. Shifts in the frequencies of these vibrations and the appearances of the additional ones, as well as their overlapping and masking by water molecule vibrations, complicate the interpretation of apatite spectra. For a better differentiation of the OH bands in FTIR spectra the Peak Fitting Program "Galactic" [5–8] was used.

* Corresponding author. Tel.: +372 6445810; fax: +372 6202801 (M. Veiderma), Tel.: +372 6202859; fax: +372 6202020 (K. Tõnsuaadu).
E-mail addresses: veiderma@akadeemia.ee (M. Veiderma), kaiat@staff.ttu.ee (K. Tõnsuaadu).

0022-328X/$ - see front matter © 2004 Elsevier B.V. All rights reserved.
doi:10.1016/j.jorganchem.2004.11.022

Samples investigated were distributed into three groups: (1) synthetic apatites obtained by precipitation from solutions as described in [6]; (2) magmatic apatites from Northern Europe; and (3) sedimentary apatites (phosphorites) of different deposits.

The effect of the chemical composition of apatites on the OH bonds can be easily demonstrated for synthetic non-stoichiometric carbonate apatites with different CO_3:PO_4 and OH:F mole ratios, containing also vacancies. The increase in the content of CO_3 groups and fluorine in apatite structure causes an increase in the number of the peaks and a change in their intensities (Fig. 1). Analysis of the OH stretching vibrations in the apatite spectra testified the existence of various OH clusters in the presence of carbonate and fluorine ions [6].

In magmatic apatites the highest content of fluorine is in Kola apatite ($n = 1.9$), the lowest in Kovdor apatite ($n = 0.6$). Sedimentary apatites are B-type carbonate apatites with mole ratio of CO_3/PO_4 in the range from 0.1 for metamorphic Karatau phosphorite to 0.3 for pebble phosphorite from Jegor'evsk deposit. The last named sample occurs as an exception, containing excess of fluorine regarding the stoichiometry, which may be explained by an existence of coupled ionic group of CO_3^{2-} and F^- [1,9].

The OH stretching mode in FTIR spectra of magmatic apatites are shown in Fig. 2(a). In the interval of 3500–3600 cm^{-1} only two OH bands are found. However, the line shape of these bands obtained by peak fitting reveals a more complicated picture (Fig. 2(b)). In the IR spectrum of the most "idealized" Kola fluorapatite, the intensive OH stretching mode is located at 3536 cm^{-1}. The weak bands at 3587 and 3567 cm^{-1} belong to OH groups that do not form a hydrogen bond with fluorine. In the spectra of Kovdor apatite three intensive OH bands at 3534, 3547 and 3568 cm^{-1} and a weak band at 3584 cm^{-1} have been found. The bands at 3534 and 3547 cm^{-1} belong to the OH stretching mode in hydrogen bond OH···F in case the amount of fluorine is, respectively, bigger or smaller than that of OH groups. The band at 3568 cm^{-1} belongs to hydrogen bond OH···O [1]. The most intensive OH stretching mode in Kiruna and Siilinjärvi (for both $n = 1.5$) apatite spectra, as well as in Kola apatite, is located at about 3537 cm^{-1}.

The IR spectra of sedimentary apatites are much more complicated (Fig. 3). In the peak-fitted spectrum of Jegor'evsk phosphorite, in which the contents of carbonate and fluorine are the highest, seven bands were

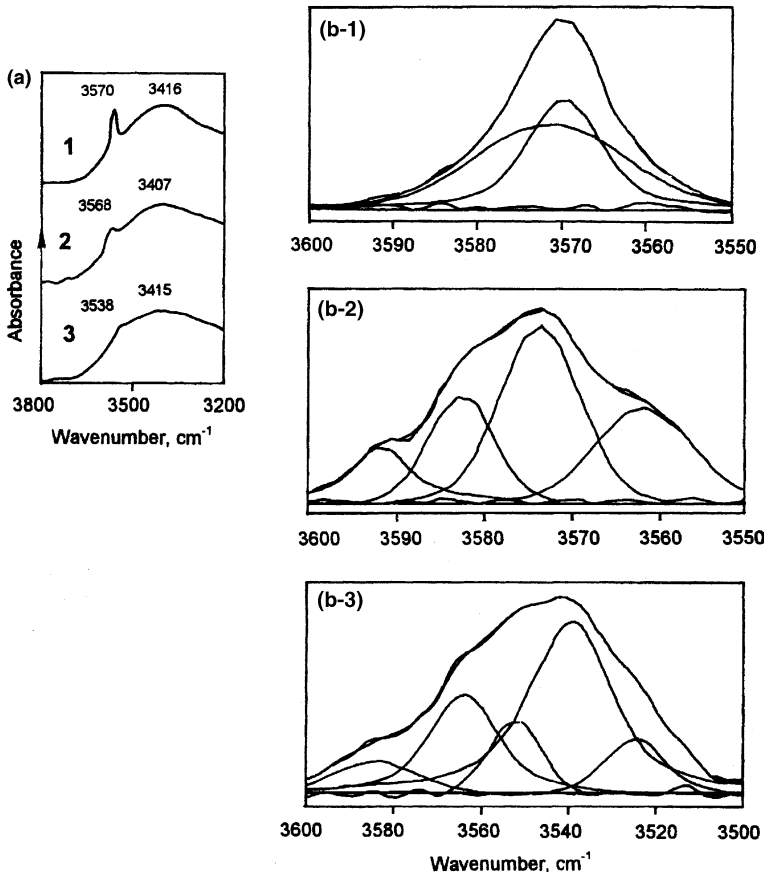

Fig. 1. FTIR spectra of synthetic apatites: 1, $Ca_{9.9 \pm 0.1}(PO_4)_{5.7}(CO_3)_{0.3}(OH)_2$; 2, $Ca_{9.6 \pm 0.4}(PO_4)_{5.1}(CO_3)_{0.9}(OH)_2$; 3, $Ca_{9.8 \pm 0.2}(PO_4)_{4.8}(CO_3)_{0.4}$-$(CO_3F)_{0.8}F_{0.9}(OH)_{1.1}$. (a) OH and H_2O bands. (b) decomposition of the OH ν_1 mode by peak fitting.

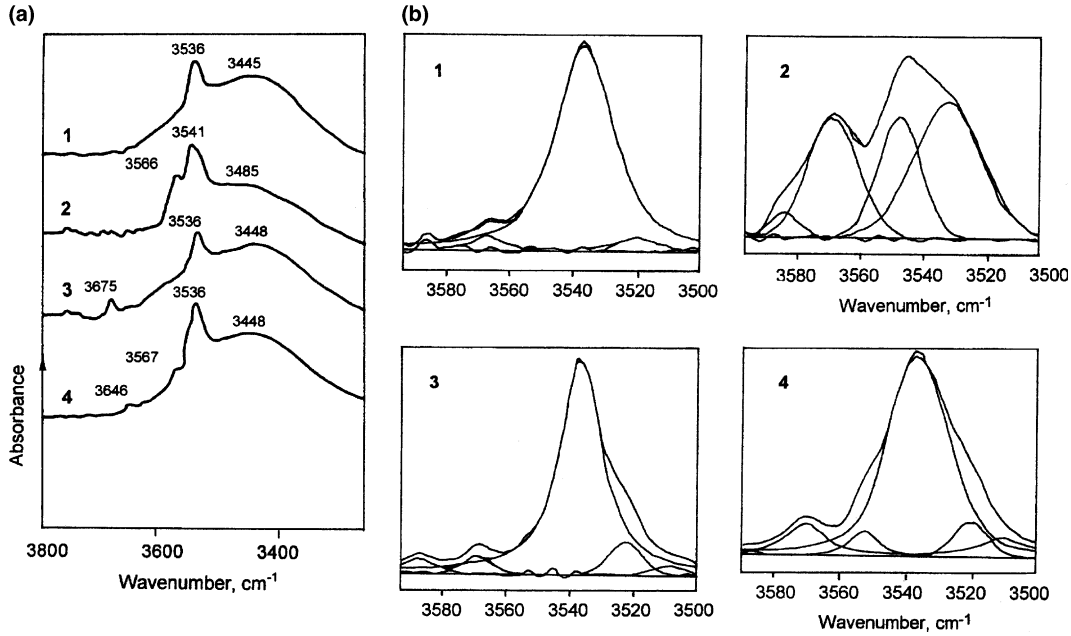

Fig. 2. FTIR spectra of magmatic apatites: (a) OH and H_2O bands in Kola (1), Kovdor (2), Kiruna (3), and Siilinjärvi (4) apatites spectra; (b) decomposition of the OH ν_1 mode by peak fitting.

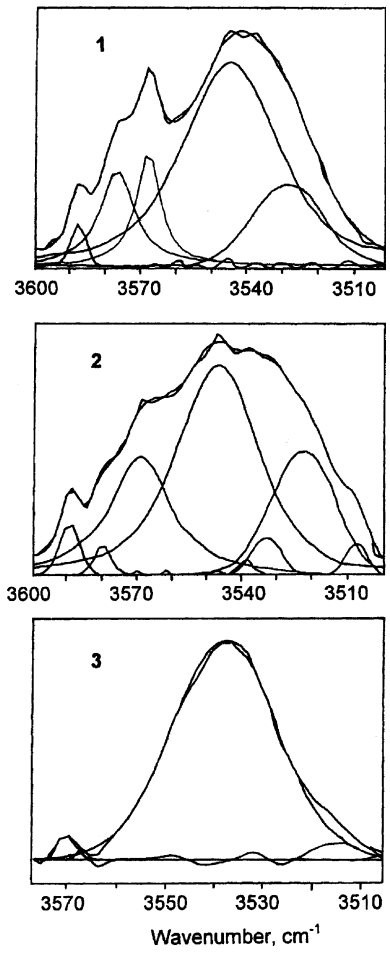

Fig. 3. Decomposition of the OH ν_1 mode by peak fitting in the FTIR spectra of phosphorites from Rakvere (1), Egor'evsk (2), and Karatau (3).

established in the domain 3500–3600 cm^{-1}. The stretching modes in Rakvere phosphorite spectrum include five bands, while the spectrum of Karatau metamorphic apatite contains only one intensive OH stretching mode at 3537 cm^{-1} and two weak bands like those in the Kola apatite spectrum. Earlier a correlation between the changes of phosphorite properties (porosity, solubility, reactivity, thermal stability, etc.) and the increase in CO_3 group content in the apatite mineral was established [9]. Thus, disturbance of the apatite structure as a result of the incorporation of CO_3 groups is expressed also by changes in OH stretching mode in the IR spectra.

3. Carbonate and sulphate substituted apatites

The structure and properties of carbonate apatite, including the existence of two positions of carbonate ion (A and B type), are well known [1,2,10–12], while sulphate apatites are poorly studied. The substitutions of CO_3 and SO_4 groups for PO_4 cause a decrease in the symmetry and stability of apatite structure. As a result of these substitutions shifts and splitting of the PO_4 vibration bands occur in the apatite IR spectra (Fig. 4). According to data of XRD analysis the unit cell parameters change – in carbonate apatite to a larger extent than in sulphate apatite, as it is shown for synthetic precipitated apatites presented in Table 1.

Differences in the structure and composition of substituted apatites become obvious also during calcination. The identification of the transformations is often

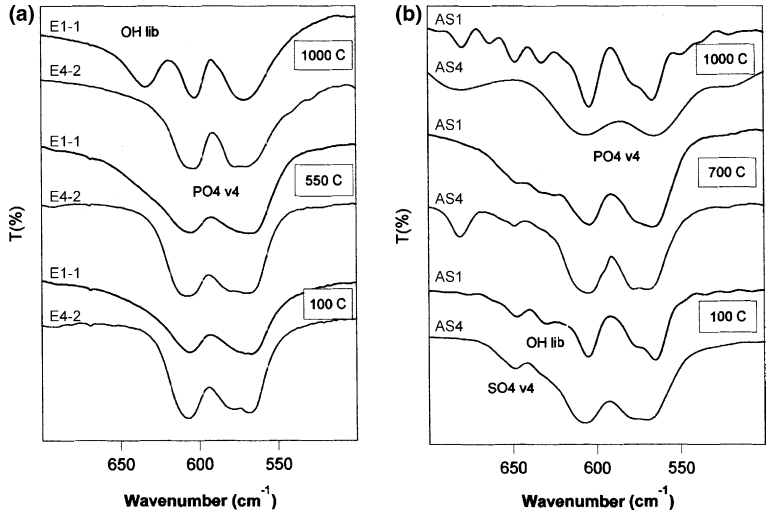

Fig. 4. OH libration, v_4 of SO_4^{2-} and v_4 of PO_4^{3-} peaks in FTIR spectra of apatites at 500–700 cm^{-1}: (a) carbonate apatites heated at 100, 550 and 1000 °C. (b) sulphate apatites heated at 100, 700 and 1000 °C. Composition of the samples is presented in Table 1.

Table 1
Composition and unit cell parameters of synthetic apatite samples

Sample	Formula	Unit cell parameters (Å)					
		$a \pm 0.001$			$c \pm 0.001$		
		Temperature (°C)					
		100	500	1000	100	500	1000
A1-1	$Ca_{9.95 \pm 0.14}(PO_4)_{5.71}(CO_3)_{0.20}(OH)_2 \cdot 2.12H_2O$	9.410	9.408	9.417	6.879	6.884	6.882
E1-1	$Ca_{9.46 \pm 0.54}(PO_4)_{5.00}(CO_3)_{1.00}(OH)_{1.92 \pm 0.08} \cdot 2.22H_2O$	9.394	9.375	9.416	6.894	6.889	6.886
AS1	$Ca_{9.34 \pm 0.66}(PO_4)_{4.79}(SO_4)_{1.04}(CO_3)_{0.16}(OH)_{1.78} \cdot 1.96H_2O$	9.427	9.416	9.417	6.879	6.883	6.878
A4-1	$Ca_{9.88 \pm 0.12}(PO_4)_{5.76}(CO_3)_{0.24}F_{1.49}(OH)_{0.51} \cdot 1.21H_2O$	9.382	9.368	9.373	6.891	6.890	6.885
E4-2	$Ca_{9.58 \pm 0.42}(PO_4)_{4.96}(CO_3)_{0.86}(CO_3F)_{0.18}F_{1.45}(OH)_{0.55} \cdot 1.14H_2O$	9.341	9.332	9.373	6.895	6.897	6.887
AS4	$Ca_{9.35 \pm 0.65}(PO_4)_{4.72}(SO_4)_{1.08}(CO_3)_{0.21}(OH)_{0.69}F_{1.31} \cdot 1.30H_2O + 0.29CaF_2$	9.386	9.376	9.374	6.882	6.885	6.883

rather difficult due to the overlapping of reactions with release of different gaseous species. For better differentiation of the reactions, in addition to XRD and IR analysis, the combination of thermal measurements (TG, DTG, and DTA) with the analysis of evolved gases (EGA) was used: first by titrimetry (TGT) [13] and later by thermo-gaschromatography (TGC) [14,15] and FTIR analysis [16]. Examples of TGC and FTIR application for a sample of non-stoichiometric synthetic apatite are presented in Fig. 5. The evolvement of H_2O, NH_3, and CO_2 and exothermic effects caused by regulation of apatite structure are observed.

In natural carbonateapatites (B-type) the evolvement of CO_2 and rearrangement of the apatite structure to more regular one proceeds in one-two steps at temperatures 600–1000 °C [17]. For nonstoichometric carbonate apatites, the transformations occur at several steps with the evolvement of H_2O and CO_2 from 150 up to 900 °C and are influenced by cationic substitutions [19]. Partial relocation of CO_3 groups into A-position on the *c*-axis was observed. Due to the excess of calcium in comparison with stoichiometric Ca-apatite the formation of CaO or CaF_2 occurs [17–19].

Thermal behaviour of precipitated synthetic sulphate apatite is different. At calcination in the range of 700–850 °C SO_4^{2-} leaves apatite structure with the formation of separate $CaSO_4$ phase [20,21]. Therefore, the mass loss is smaller than in the case of carbonate apatite (Fig. 6).

As a result of thermal treatment up to 1000 °C both carbonate and sulphate apatites acquire the same unit cell parameters close to those of stoichiometric OH- or F-apatites (Table 1). The formation of stoichiometric OH- or F-apatites is confirmed also by IR spectroscopy (Fig. 4).

It is essential to note that $CaSO_4$ (together with $Ca_2P_2O_7$) is formed also when apatite is calcined in the SO_2 – air flow above 400 °C as it was shown in [22,23]

$$Ca_{10}(PO_4)_6F_2 + 4SO_2 + 2O_2 \rightarrow 4CaSO_4 + 3Ca_2P_2O_7 + 2HF$$

A reaction between $CaSO_4$ and $Ca_2P_2O_7$ occurs at temperatures 880–1000 °C resulting in evolvement of SO_3 and formation of β-$Ca_3(PO_4)_2$ or its solid solution with $CaSO_4$ similar to calcium phosphosulphate described by Marraha et al. [24]

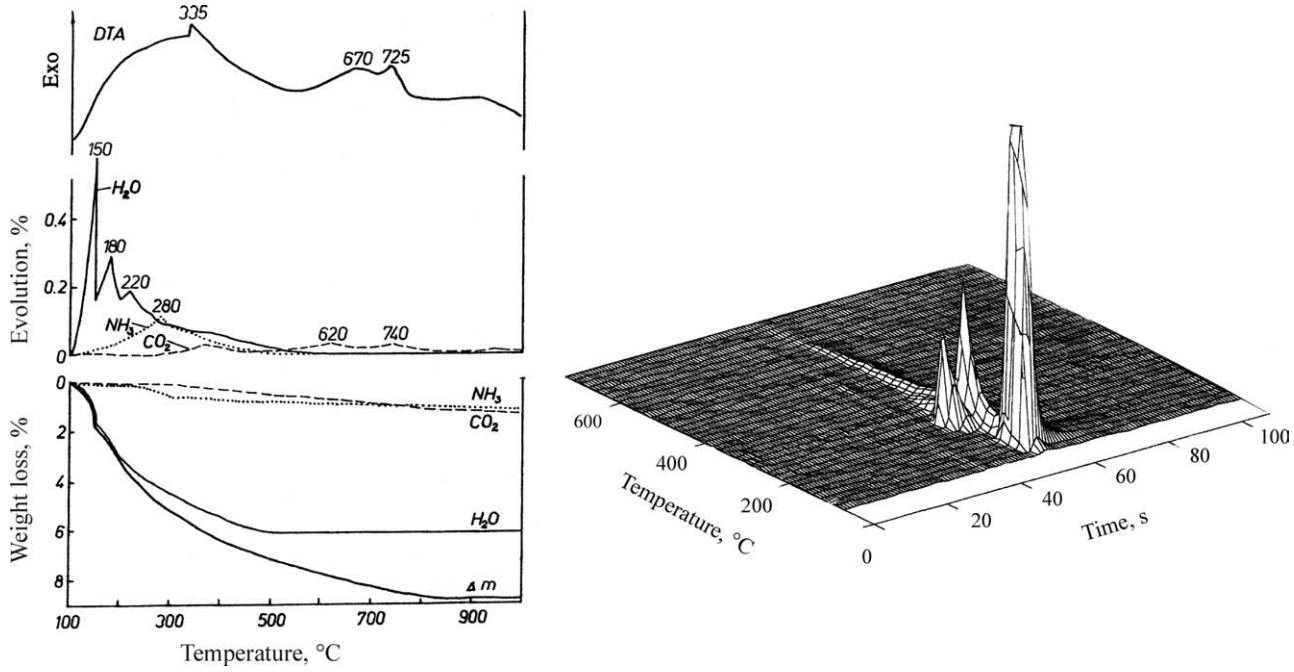

Fig. 5. Thermoanalytical curves of the apatite sample $Ca_{6.37}Mg_{2.70}(NH_4)_{0.88}(HPO_4)_{0.56}(PO_4)_{5.02}(CO_3)_{0.42}F_{1.43}(OH)_{0.57} \cdot 3.08H_2O$: (a) TG–EGA by FTIR; (b) by thermo-gas chromatography.

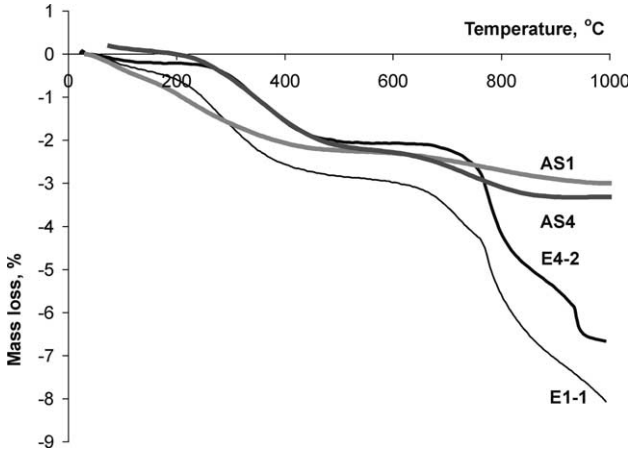

Fig. 6. Mass loss of the apatite samples E1-1, E4-2, AS1, and AS4 at heating up to 1000 °C.

$$CaSO_4 + Ca_2P_2O_7 \rightarrow Ca_3(PO_4)_2 + SO_3$$

The amount of SO_2 bound with apatite and the rate of the reaction depends much on the stability of apatite structure. At isothermal heating of carbonate apatite at 550° when the structure of apatite is in most irregular state before CO_2 separation the reaction yield is the biggest. At higher temperatures the more regular structure forms and the reaction extent with SO_2 decreases (Table 2).

Table 2
Composition of carbonate apatite E4-2 calcined in the air + SO_2 (10%) flow during 1 h

Temperature (°C)	550	700	800
SO_3 (%)	27.7	17.0	13.7
F (%)	0.5	1.4	2.1
F evolved (rel.%)	79.4	40.1	19.9

Acknowledgements

The help provided by V. Bender, M. Koel, M. Einard and A. Manuilova in carrying out XRD, thermo-gas chromatography, and chemical analyses, respectively, is gratefully acknowledged.

References

[1] J.C. Elliot, Structure and Chemistry of Apatites and Other Calcium Orthophosphates, Elsevier, 1994, p. 389.
[2] J.C. Elliot, in: Calcium Phosphate Materials. Fundamentals, Sauramps Medical, 1998, pp. 25–26.
[3] C. Rey, Phosphorus Res. Bull. 1 (1991) 1.
[4] M. Veiderma, M. Pyldme, K. Tynsuaadu, Chemische Technik 40 (1988) 169.
[5] Galactic peaksolve, Peak Fitting for WindowsUser's Guide, Galactic Industries Corporation, USA, 1995, p. 225.
[6] R. Knubovets, M. Veiderma, K. Tõnsuaadu, Proc. Estonian Acad. Sci. Chem. 47 (1998) 163.
[7] M. Veiderma, R. Knubovets, K. Tõnsuaadu, Bull. Geol. Soc. Finland 70 (1998) 69.
[8] R. Knubovets, Rev. Chem. Eng. 9 (1993) 161.
[9] M. Veiderma, Proc. Estonian Acad. Sci. Chem. Geol. 26 (1977) 28.
[10] M. Vignoles, G. Bonel, G. Bacquet, Bull. Mineral. 105 (1982) 307.

[11] M. Jemal, I. Khattech, Thermochim. Acta 152 (1989) 65.
[12] J.P. Lafon, E. Champion, D. Bernache-Assollant, R. Gibert, A.M. Danna, J. Therm. Anal. Cal. 73 (2003) 1127.
[13] T. Kaljuvee, M. Veiderma, K. Tynsuaadu, H. Vilbok, J. Therm. Anal. Cal. 33 (1988) 839.
[14] M. Koel, M. Kudrjashova, K. Tõnsuaadu, M. Peld, M. Veiderma, Thermochim. Acta 322 (1998) 25.
[15] K. Tõnsuaadu, M. Koel, M. Veiderma, J. Therm. Anal. Cal. 64 (2001) 1247.
[16] K. Tõnsuaadu, M. Peld, T. Leskelä, R. Mannonen, L. Niinistö, M. Veiderma, Thermochim. Acta 256 (1995) 55.
[17] H. Vilbok, R. Knubovets, M. Veiderma, Proc. Estonian Acad. Sci. Chem. 41 (1992) 45.
[18] K. Tõnsuaadu, M. Peld, V. Bender, Phosphorus Res. Bull. 14 (2002) 89.
[19] K. Tõnsuaadu, M. Peld, V. Bender, J. Therm. Anal. Cal. 72 (2003) 363.
[20] K. Tõnsuaadu, M. Peld, M. Quarton, V. Bender, M. Veiderma, Phosphorus, Sulfur, Silicon 177 (2002) 1873.
[21] K. Tõnsuaadu, M. Peld, V. Bender, M. Veiderma, J. Therm. Anal. Cal. 56 (1999) 35.
[22] M. Veiderma, K. Tõnsuaadu, M. Peld, V. Bender, Phosphorus Res. Bull. 10 (1999) 256.
[23] A. Manuilova, K. Tõnsuaadu, M. Veiderma, Phosphorus Res. Bull. 14 (2002) 93.
[24] M. Marraha, J.C. Heughebaert, M. Heughebaert, Phosphorus, Sulfur, Silicon 79 (1993) 281.